Ion Mass Dependence of Resistive Drift Wave Turbulence in Cylindrical Plasmas

Naohiro KASUYA[1,2], Masanobu ISHIDA[2], Yudai IMAHASHI[2] and Masatoshi YAGI[3]

[1])*Research Institute for Applied Mechanics, Kyushu University, Kasuga, Fukuoka 816-8580, Japan*
[2])*Interdisciplinary Graduate School of Engineering Sciences, Kyushu University, Kasuga, Fukuoka 816-8580, Japan*
[3])*National Institute for Quantum and Radiological Science and Technology, Obuchi, Rokkasho-mura, Aomori 039-3212, Japan*

Resistive drift wave instability is one of the driving sources of turbulence in linear devices, and its ion mass dependence on structural formation is investigated by turbulence simulation. Modes are less unstable in the case with smaller mass ions, because the normalized density gradient length becomes larger with larger Larmor radius, but can be unstable considering the change of ion-neutral collision frequency. Nonlinear calculations show that a large number of modes with larger axial mode numbers are linearly unstable and their nonlinear couplings induce turbulence with a zonal flow in the case of smaller mass ions as helium.

Since turbulence structures have great influence on plasma transport [1], understanding of their formation mechanism is important for the control of fusion plasmas. Experiments in linear device PANTA have shown that there exist several types of nonlinear structures generated by drift wave instabilities, depending on parameters [2], such as streamers [3], zonal flows and solitary drift waves [4]. Numerical simulations also have shown structural bifurcation [5, 6]. On the other hand, it is known that the change of ion mass number leads turbulence suppression in fusion plasmas [7]. In this study, we perform numerical simulations for the linear device using turbulence code Numerical Linear Device (NLD) [8]. NLD code has been used for comparison of drift wave turbulence with linear device experiments, and show good agreements in unstable mode characteristics as the spectrum and radial structure [3, 6, 9]. Difference of nonlinear saturation states of resistive drift wave instability is illuminated by changing discharge gas here.

The target of this study is PANTA device in Kyushu University, which produces a cylindrical plasma with homogeneous magnetic fields in the axial direction. Resistive drift wave instability in PANTA plasmas is calculated using the following three-field reduced fluid equations [8];

$$\frac{dN}{dt} = -\nabla_\parallel V - V\nabla_\parallel N + \mu_N \nabla_\perp^2 N + S, \qquad (1)$$

$$\frac{d\nabla_\perp^2 \phi}{dt} = \nabla N \cdot \left(-\nu_{in}\nabla_\perp \phi - \frac{d\nabla_\perp \phi}{dt} \right) - \nu_{in}\nabla_\perp^2 \phi$$
$$- \nabla_\parallel V - V\nabla_\parallel N + \mu_W \nabla_\perp^4 \phi, \qquad (2)$$

author's e-mail: kasuya@riam.kyushu-u.ac.jp

$$\frac{dV}{dt} = \frac{M}{m_e}(\nabla_\parallel \phi - \nabla_\parallel N) - (\nu_{ei} + \nu_{en})V + \mu_V \nabla_\perp^2 V, \qquad (3)$$

where N is the density, ϕ is the electrostatic potential, V is the electron velocity in the magnetic field direction, S is the particle source, ν is the collision frequency, and μ is the viscosity. The time and distance are normalized by the ion cyclotron frequency Ω_{ci} and the effective Larmor radius $\rho_s = \sqrt{MT_e}/eB$ evaluated by using the electron temperature T_e, respectively. Neutral particles exist even in the center of this rather low temperature plasma, so the effect of neutrals is included by the ν_{in} terms. In addition, only charge number Z = +1 ions are considered in the following calculations.

The set of model Eqs. (1-3) is solved for a plasma with a cylindrical shape. The boundary conditions are given as a periodic boundary in the axial direction, and zero fluctuations at the plasma center and outer boundary in the radial direction. The mean components are also calculated in the nonlinear simulations, which have the boundary conditions that their derivative is zero at the plasma center.

The simulation parameters are the followings; magnetic field $B = 0.1$ T, electron temperature $T_e = 3$ eV, plasma radius $a = 7$ cm, device axial length $\lambda = 4$ m, electron-ion collision frequency $\nu_{ei}/\Omega_{ci} = 300$, electron-neutral collision frequency $\nu_{en}/\Omega_{ci} = 10$, viscosities $\mu_W = \mu_V = 10^{-4}, \mu_N = 10^{-2}$. Note that the perturbation is zero at $r = a$ with the boundary condition of the calculation.

First, a linear analysis of eigen modes is performed. The model equations are linearized, and the radial mode structure and the eigen values are calculated for each mode with azimuthal mode number m and axial mode number n. Using the PANTA device parameters, the cases with

discharge gas argon (Ar), neon (Ne), and helium (He) are analyzed. The fixed background density profile with

$$N = N_0 \left[\exp\left(-\left(\frac{r}{L_{N1}}\right)^2 \right) - 1 \right], \qquad (4)$$

is used, where the strength is $N_0 = 4.0$ and the characteristic length L_{N1} is given with the plasma radius as $L_{N1} = a/\rho_s$. Length L_{N1} is normalized by ρ_s, so is larger with smaller mass number. The drive of the instability is the density gradient, so larger L_{N1} gives smaller linear growth rate. Figures 1 (a-c) show the linear growth rate dependence for Ar, Ne and He. The same collision frequency ν_{in} is used to check the influence of different mass numbers. In these cases, there are unstable modes with rather smaller m and n as indicated by the dashed lines. In the He case, the linear growth rates in the wide (m, n) region increases, but are less than zero. The maximum of the growth rate for He is also smaller than the cases for Ar and Ne. Actually, the collision frequencies are different for different ion species. By considering the effective radius of atoms, ν_{in} of He is smaller than those of Ne and Ar. Figure 1 (d) show the case of He with smaller ν_{in}. The unstable modes exist in the wider range. This is due to the dependency on ρ_s. If modes with the same range of $k\rho_s$ become unstable, the mode number and a number of unstable modes are approximately scales to ρ_s^{-1}, so a larger number of unstable modes exist in the He case.

Next, nonlinear calculations are performed for resistive drift wave turbulence. Flux driven simulations are carried out with a time-independent particle source

$$S_N(r) = \frac{4S_0\mu_N}{L_{N2}^2}\left[1 - \left(\frac{r}{L_{N2}}\right)^2\right]\exp\left[-\left(\frac{r}{L_{N2}}\right)^2\right], \quad (5)$$

where S_0 is the intensity of the source and L_{N2} gives the scale length of the density profile without fluctuations. The ba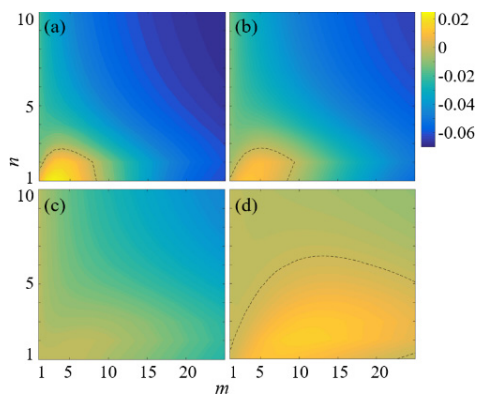ckground density profiles are determined self-consistently with this particle source, so are different from that in Eq. (4). Figure 2 (a) shows the time evolutions of the mode energy in the case of He with $\nu_{in} = 0.01$, $S_0 = 10$, $L_{N2} = a$. In the linear phase, the modes around $(m, n) = (7, 4)$ are excited (Fig. 3 (a)), and their mode couplings give the nonlinear saturation. The energy of the unstable modes is transferred to the other modes, and a wide range of modes have the same level of amplitudes, resulting a turbulent state (Fig. 3 (b)). A zonal flow with $(m, n) = (0, 0)$ is also excited. On the other hand, in the Ar case with $\nu_{in} = 0.1$, $S_0 = 5$, $L_{N2} = a$, modes with $(m, n) = (2, 1)$ and $(3, 1)$ become unstable in the linear phase, and are still dominant in the nonlinear phase (Fig. 2 (b) and Figs. 3 (c, d)). Those higher harmonics are also excited, but the limited number of modes are dominant. The linear analysis as in Fig. 1 predicts that the number of unstable modes is larger in the He case. The difference in the mode spectra arise in spite of nonlinear relaxation of the background density profile. Nonlinear calculations are carried out for the Ne case, and the rather small difference gives the same kind of nonlinear state with the Ar case.
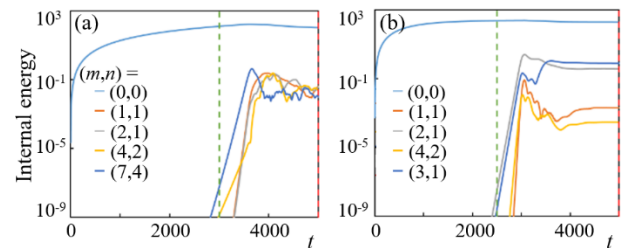

Fig. 2 Time evolutions of internal energy of each mode. The cases of (a) He with $\nu_{in} = 0.01$ and (b) Ar with $\nu_{in} = 0.1$ are shown. The $(m, n) = (0, 0)$ component indicates the evolution of the background plasma density.
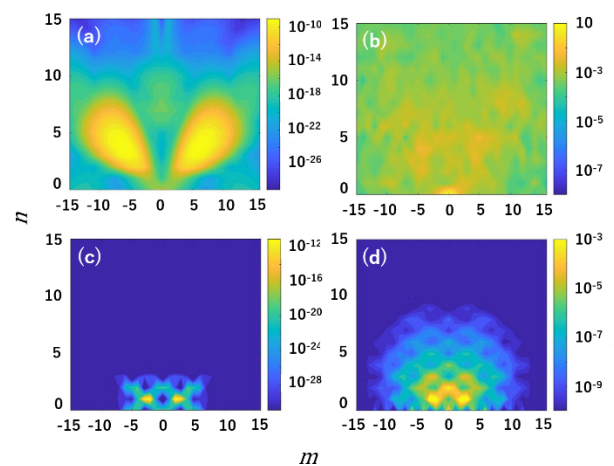

Fig. 1 Linear growth rate of resistive drift wave instability for each ion species ((a) Ar, (b) Ne, (c) He with $\nu_{in} = 0.06$, and (d) He with $\nu_{in} = 0.01$). The dependencies on mode numbers m and n are shown. The dotted line indicates the unstable boundary with zero growth rate.

Fig. 3 $m - n$ mode spectra of the (a) linear and (b) nonlinear phase in Fig. 2 (a), and the (c) linear and (d) nonlinear phase in Fig. 2 (b).

In this research, the ion mass dependence of the resistive drift wave instability was investigated. The difference in the characteristic length and collision frequency for the different ion species leads the difference in the nonlinear structure. In PANTA, previous experiments and simulations are mainly carried out for Ar discharges, and experiments with He discharges are ongoing. We will investigate the characteristics in mode spectra and turbulent states obtained in this analysis by comparing with experiments.

[1] P.H. Diamond *et al.*, Plasma Phys. Control. Fusion **47**, R35 (2005).
[2] T. Kobayashi *et al.*, Plasma Fusion Res. **12**, 1401019 (2017).
[3] T. Yamada *et al.*, Nature Phys. **4**, 721 (2008).
[4] H. Arakawa *et al.*, Plasma Phys. Control. Fusion **53**, 115009 (2011).
[5] N. Kasuya *et al.*, Phys. Plasmas **15**, 052302 (2008).
[6] M. Sasaki *et al.*, Phys. Plasmas **22**, 032315 (2015).
[7] M. Nakata *el al.*, Phys. Rev. Lett. **118**, 165002 (2017).
[8] N. Kasuya *et al.*, J. Phys. Soc. Jpn. **76**, 044501 (2007).
[9] T. Yamada *et al.*, Plasma Fusion Res. **8**, 2401022 (2013).